A Power Amplifier for Millimeter-Wave 5G Base Stations Covering 24−30 GHz

Chihiro Kamidaki,[1] Yuma Okuyama,[1] Tatsuo Kubo,[1] Yo Yamaguchi,[1] and Ning Guan[2]

In this paper, we present a millimeter-wave-band power amplifier (PA) for the 5th generation of mobile technology (5G) base stations. The PA adopts an output matching network with integrated transmission/reception switches to support time-division duplexing, while being designed to maximize the saturated output power (P_{sat}) and power-added efficiency (PAE) and higher linearity (i.e. lower AM-AM distortion) in the n257, n258, and n261 frequency bands specified by the 5G NR. The PA fabricated in a 130-nm SiGe BiCMOS process demonstrates a maximum gain of 30.3 dB and a 3-dB bandwidth of 9.8 GHz, and it achieves a P_{sat} over 20 dBm, a PAE of over 22%, and an AM-AM distortion of less than 0.1 dB in the 24−30 GHz range. The figure of merit of International Technology Roadmap for Semiconductors (ITRS FoM) calculated from these parameters reaches competitive value of 93.3. Furthermore, in modulation signal measurements, the PA demonstrates an output power of 12.3 dBm, a PAE of 8.8%, and an adjacent channel power ratio of −32.7 dBc when the error vector magnitude is −25 dB (5.6%).

1. Introduction

The 5th generation of mobile technology (5G) has been launched in many countries all over the world since 2019. In order to meet continuously growing demand for communication by users, base stations in the n257 (26.5−29.5 GHz), n258 (24.25−27.5 GHz), and n261 (27.5−28.35 GHz) frequency bands specified in the 5G NR are being installed to provide services in the millimeter-wave band and enhance communication speed and capacity [1]. However, the communication distance with a single antenna gets shorter as the carrier frequency increases in wireless communications due to the loss increase in free-space propagation. Also, the communication direction is constrained due to the difficulty of diffraction at high frequency.

Phased array antenna module (PAAM) [2] is a module consists of multiple integrated circuits (ICs) of beamformer IC (BFIC) and frequency conversion IC (FCIC) [3], passive components such as a bandpass filter [4] and combiner/splitter, and an Antenna-in-Package (AiP) [5]. The FCIC receives baseband signal and converts to millimeter-wave signal, which is then distributed to multiple BFICs through bandpass filters and combiners/splitters. The BFIC controls phase and amplitude of the millimeter-wave signal and emits to radio waves from the array antenna to achieve beamforming, which extends communication distance and controls direction. It allows PAAM users to control the propagation of millimeter-waves while avoiding direct handling.

Power amplifier (PA) is one of the key circuits in the BFIC, which is connected to the antenna through the transmission/reception switch (TRX SW) when the PAAM is in transmission (TX) mode. PA performance requirements vary widely. Increasing the output power of the PA is an effective way to increase the equivalent isotropic radiated power (EIRP) of the PAAM to further extend the communication distance. It is also important to improve the linearity of the PA, expressed in terms of amplitude-amplitude distortion (AM-AM distortion) and amplitude-phase distortion (AM-PM distortion), to deliver higher communication quality to distant people as multicarrier transmission and higher-order phase-amplitude modulation are applied in 5G communications [6] . In addition, there is a demand to improve the power added efficiency (PAE) of the PA, which accounts for a large proportion of the power consumption of the BFIC [7]. Finally, by achieving these performances in the frequency range of 24.25−29.5 GHz, the number of manufacturing varieties can be reduced to lower management costs.

In this paper, a PA with a saturation output power (P_{sat}) exceeding 20 dBm in the frequency range from 24 to 30 GHz is presented. The PA is designed with an output matching circuit including a TRX SW and a low noise amplifier (LNA) to be used in time-division-duplex (TDD) mode. The PA shows high linearity and efficiency in continuous wave (CW) measurements and competitive Figure of Merit (FoM) defined by International Technology Roadmap for Semiconductors (ITRS). Finally, measurements with modulated signals show that the PA delivers high power while maintaining a low error vector magnitude (EVM).

1 : Millimeter-wave Device Research Department

2 : Electronic Technologies R&D Center

Abbreviations, Acronyms, and Terms.

5G—Fifth Generation Mobile Communication System
The fifth-generation technology standard for broadband cellular networks.

5G NR—5G New Radio
A new radio access technology for the fifth-generation network.

TDD—Time Division Duplex
A telecommunications technology that enables communication in the same frequency band by switching between transmission and reception.

PAE—Power Added Efficiency
A ratio of increased signal power and supplied DC power.

AM-AM distortion—Amplitude Modulation - Amplitude Modulation distortion
A nonlinear response of the magnitude of output power to the input power.

BiCMOS—Bipolar CMOS
A semiconductor technology that enables the use of both bipolar transistors and CMOS transistors.

BW_{3dB}—3-dB bandwidth
The bandwidth of frequencies at outside of which the signal amplitude reduces by 3 dB from its maximum value.

EVM—Error Vector Magnitude
A measure used to quantify the performance of a modulation signal, calculated as the ratio of the root mean square values of the ideal signal vector and the error vector.

ACPR—Adjacent Channel Power Ratio
A ratio of the total power of the adjacent channel to the power of the main channel.

PAAM—Phased Array Antenna Module
A module consisted of phased array annte-na, BFIC, FCIC, filters and combiners/splitters.

BFIC—Beamformer IC
An integrated circuit that emits radio waves with appropriate phase to array antenna for transmitting or receiving signal from or to desired directions.

FCIC—Frequency Conversion IC
An integrated circuit that converts signal with certain frequencies to that with different frequencies.

AiP—Antenna in Package
A structure in which high-frequency integrated circuits, antennas, and other components are integrated.

Array antenna—Array antenna
An array of antenna elements with the same shape. The radiation direction can be controlled by adjusting the phase and amplitude of the signal from each element.

AM-PM distortion—Amplitude Modulation - Phase Modulation Distortion
The nonlinear response of the phase of output power to the input power.

EIRP—Equivalent Isotropic Radiated Power
A parameter measuring the gain of an antenna, is defined by the product of the input power and the maxiumu gain.

LNA—Low Noise Amplifier
An amplifier characterized by its ability to amplify weak signals while keeping the generated noise low.

P_{sat}—Saturated Output Power
Output power when the amplifier is saturated.

oP_{1dB}—Output 1-dB Compression Point
A measure of the linearity of an amplifier, is the output power starts to drop off 1 dB from the linear input/output power curve.

Smith Chart—Smith Chart
A graph of the reflection coefficient displayed in a polar coordinate, with equal-resistance circles and equal-reactance circles indicated.

S Parameter—Scattering Parameter
A parameter that indicates the performance of a high-frequency circuit.

QAM—Quadrature Amplitude Modulation
A modulation method that transmits a signal by adjusting the amplitude of two carrier waves that are independent and in quadrature with each other. A type of digital modulation method that transmits data by modulating both amplitude and phase.

OFDM—Orthogonal Frequency Division Multiplexing
A type of multi-carrier modulation in which the phases of subcarriers of adjacent frequencies are orthogonalized to transmit signals with some of the subcarrier spectra overlapping.

CMOS—Complementary MOS
A semiconductor circuit based on P-type and N-type MOS transistors, or its manufacturing technology.

SOI—Silicon On Insulator
A semiconductor structure consisting of an oxide insulating layer under the MOS transistor for improving performance by increasing speed and reducing power consumption.

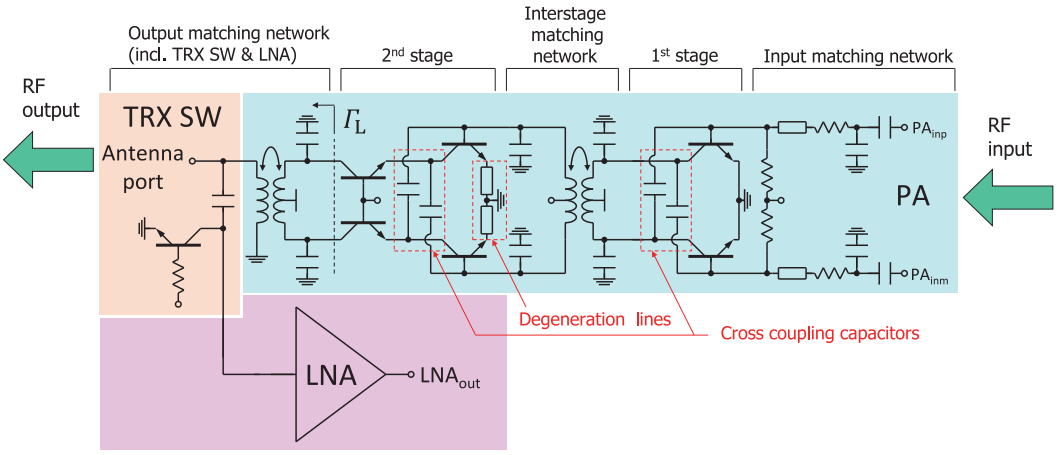

Fig. 1. Schematic diagram of proposed PA with LNA and TRX SW.

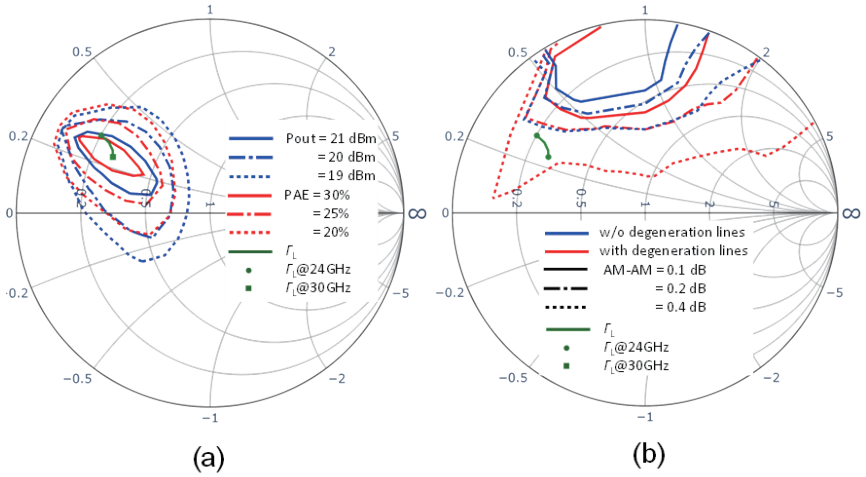

Fig. 2. (a) Pout and PAE contour of the PA at 28 GHz. (b) AM-AM contour of the PA at 28 GHz.

2. Circuit Design

The schematic of the proposed PA with co-designed LNA and TRX SW is shown in Figure 1. The first and second stages of the PA are configured as a differential common-emitter amplifier and a differential cascode amplifier, respectively. They are connected by an interstage matching circuit using a transformer to achieve a wide frequency bandwidth. Each stage is equipped with a cross-coupling capacitor to neutralize the parasitic capacitance of the transistors for improved stability. The emitter of the common-emitter transistors in the second stage are connected to a degeneration line to provide negative feedback to the RF signal to suppress distortion and improve linearity at the expense of reduced gain.

Figure 2(a) shows the contour plots of the PA output power (Pout; blue) and PAE (red) at 28 GHz obtained from the load-pull simulation. In the load-pull simulation, the output matching circuit is replaced by a port with an arbitrary value of the reflection coefficient, and the output power from the second stage is analyzed with the reflection coefficient varied. Figure 2(a) also shows the input impedance (Γ_L ; green) of the output matching circuit (including TRX SW, LNA, and antenna port) from 24–30 GHz seen from the second stage. The Γ_L is plotted in the region where Pout from the second stage is above 21 dBm. This observation indicates a constant output power within the frequency range of interest. Furthermore, the contours of Pout and PAE overlap well, suggesting that both performances can be maximized simultaneously. Figure 2(b) shows the AM-AM distortion contour plots obtained by varying the reflection coefficient of the port and input power in the load-pull simulation. Here, the AM-AM distortion is calculated as the difference between the maximum gain and small-signal gain as the input power is varied. The presence of the degeneration line extends the region where AM-AM distortion is suppressed, and the Γ_L plot is included in the region where the AM-AM distortion is less than 0.4 dB.

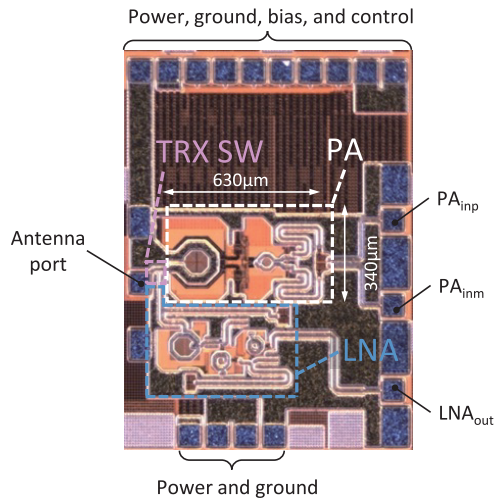

Fig. 3. Micrograph of implemented circuits fabricated in 130-nm SiGe BiCMOS process.

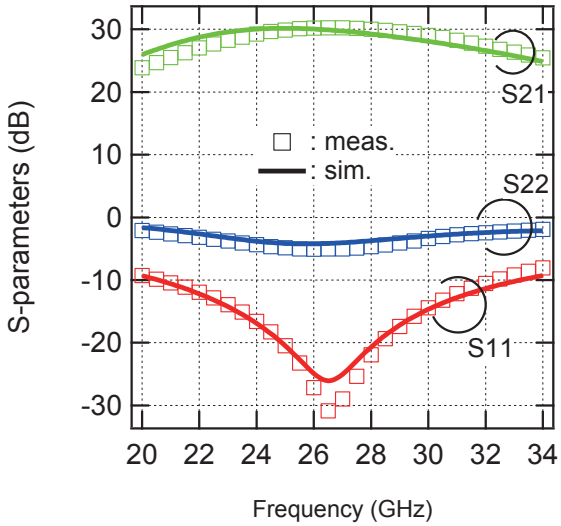

Fig. 4. Comparison of measured and simulated S-parameters of the PA.

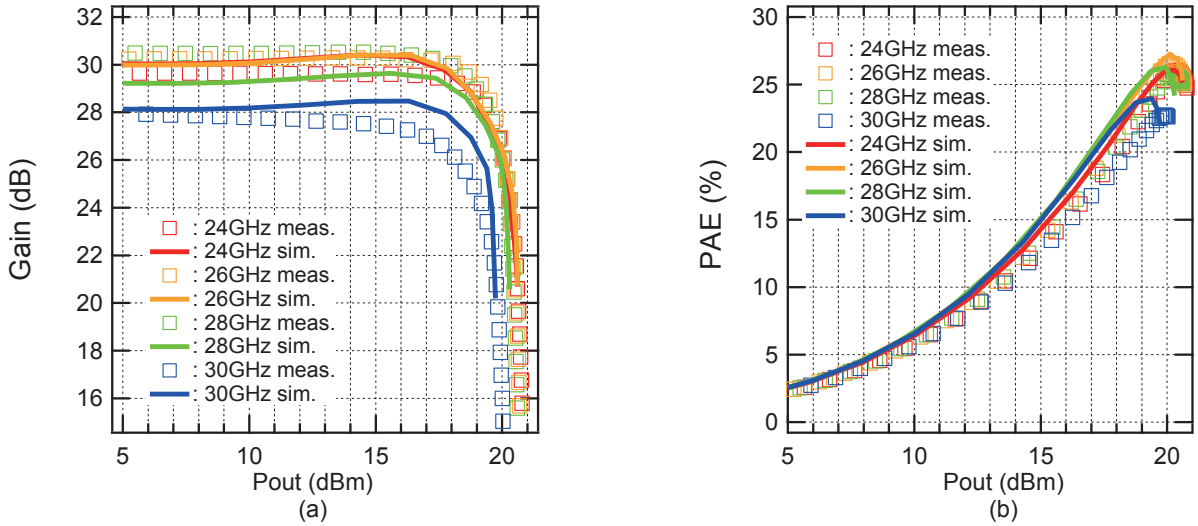

Fig. 5. CW large-signal measurement and simulation. (a) Gain. (b) PAE. [9]

3. Measurement Results

Figure 3 shows a micrograph of the circuit fabricated in 130-nm SiGe BiCMOS technology. The PA core occupies area of 0.63 mm × 0.34 mm. Figure 4 compares the measured and simulated results of the S-parameters in TX mode. The measurement results are obtained using the Keysight N5247A Vector Network Analyzer. The detailed electromagnetic field modeling and parasitic extraction in the design resulted in good agreement between the measured and simulated results. In the measurement, the PA demonstrates S_{11} of <−10 dB from 20.6 to 33.2 GHz, peak S_{21} of 30.3 dB at 26.7 GHz, 3-dB bandwidth (BW_{3dB}) of 9.8 GHz from 22.2 to 32.0 GHz.

Figures 5(a) and 5 (b) compare the measured and simulated CW large-signal response of gain and PAE, respectively, at 24, 26, 28, and 30 GHz. The input signal is generated from an E8257 Signal Generator while the output power is monitored using a Keysight N8487A Power Sensor. Overall, the measurement and simulation results are in good agreement. Figure 6 shows P_{sat}, 1-dB compression point (oP_{1dB}), PAE peak (PAE_{peak}), AM-AM distortion, and calculated ITRS FoM in the measurement and simulation at each frequency. The PA demonstrates P_{sat} >20 dBm from 24 to 30 GHz. Assuming an output matching circuit loss of 1 dB, this is consistent with the estimate from the Pout contour shown in Fig. 2(a). Similarly, assuming the Pout is reduced from 21 dBm to 20 dBm, the PAE is calculated to be reduced from 30% to 24%, which is approximately consistent with the measured results. Figure 7 (a) and (b) show the measurement results of the output spectrum and constellation of the PA using 400-MHz bandwidth and 64-QAM OFDM modulation signals at 28 GHz, respectively. In the modulation signal measurement, the input modulation signal was generated by Keysight VXG Signal Generator M9384B. The output signal of the PA was divided in two and one goes travel to Keysight UXA Signal Analyzer N9040B to measure the constellation and spectrum, and the other to Keysight N8487A to monitor the output power. The average output power, PAE, and adjacent channel power ratio (ACPR) were 12.3 dBm, 8.8%, and −32.7 dBc, respectively, at −25 dB (5.6%) EVM. Table 1 summarizes the comparison of performance of the proposed PA with the PAs reported in recent years. Despite of the fact that only the proposed PA includes TRX SW, it showed the highest ITRS FoM.

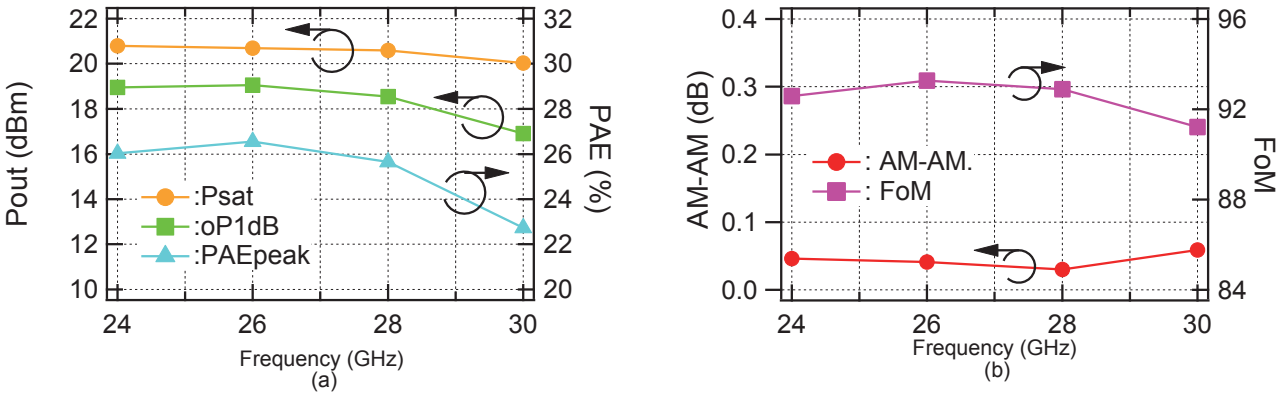

Fig. 6. Measured performances of the proposed PA. (a) P_{sat}, oP_{1dB}, PAE_{peak} (b) AM-AM, ITRS FoM

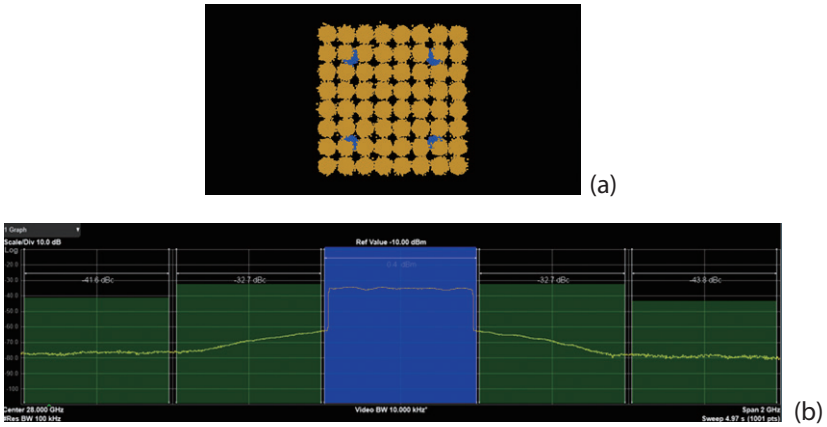

Fig. 7. Measurement results of (a) constellation and (b) output spectrum and using 64-QAM OFDM signals at 28 GHz with bandwidth of 400 MHz at EVM = –25 dB [8)9)].

Table 1. Comparison of PA performances [8)9)].

	This Work				[6] ISSCC 2018	[11] RFIC 2021	[7] JSSC 2016	[10] IMS 2020	[12] PAWR 2022
Technology	130-nm SiGe				130-nm SiGe	130-nm SiGe:C	28-nm Bulk CMOS	28-nm Bulk CMOS	45-nm SOI CMOS
Topology	Dif. 2-stage CE+CC with TRX SW				Dif. 2-stage CE+CE	Dif. 1-stage CC	Dif. 2-stage CS+CS	Dif. 2-stage CS+CS	1-stage 4-stacked-FET, Adaptive cap. & bias
BW_{3dB} [GHz]	22.2—32.0				19.0—29.5*	23.5—34.0	27.35—31.2	—	—
Frequency [GHz]	24	26	28	30	28.5	28	30	28	25
Gain [dB]	30.0	30.0	29.3	28.1	20.0	19.4	15.7	18.5	17.6
P_{sat} [dBm]	20.8	20.7	20.6	20.0	17.0	22.7	14.0	18.9	21.5
oP_{1dB} [dBm]	19.0	19.1	18.6	16.9	15.2	22.1	13.2	18.5	—
PAE_{max} [%]	26.0	26.5	25.6	22.7	43.5	38.1	35.5	39.7	39.0
FoM**.	***92.6***	***93.3***	***92.9***	***91.2***	***82.5***	***86.9***	***74.7***	***82.3***	***83.2***
Active area [mm^2]	0.21				0.29	0.16	0.16	0.31	0.22
Modulation signal	64-QAM OFDM				64-QAM OFDM	64-QAM OFDM	64-QAM OFDM	64-QAM OFDM	—
EVM [dBc].	−25				−25	−25.2	−25	−25.4	—
Pout@EVM [dBm].	12.3				9.8	16.2	4.2	9.3	—

* Pout 1-dB Bandwidth

** ITRS FoM=P_{sat} (dBm)+Gain (dB)+10 $\log_{10}$(PAE_{max} [%])+20 $\log_{10}$(Frequency [GHz]) [13].

4. Conclusion

In this paper, we present a linear broadband PA for 5G applications. The PA was fabricated in a 130-nm SiGe BiCMOS process, and shows P_{sat} >20 dBm, AM-AM distortion <0.1 dB, PAE between 22% to 27% in CW test in the frequency band of 24−30 GHz, which covers the n257, n258, and n261 frequency bands specified in 5G NR. In the modulated signal measurement using 64-QAM OFDM signal, the output power, PAE, and ACPR of PA were 12.3 dBm, 8.8%, and −32.7 dBc, respectively at −25 dB EVM at 28 GHz. It demonstrates the proposed PA is useful for highly efficient and quality communications. The ITRS FoM of 93.3 at 26 GHz is superior to the previously reported PAs.

References

1) 3GPP, 5G NR specs, http://www.3gpp.org/DynaReport/38-series.htm
2) B. Sadhu et al.: “A 24-to-30 GHz 256-element dual-polarized 5G phased array with fast beam-switching support for >30,000 beams," Proc. IEEE Int. Solid-State Circuit Conf. (ISSCC), pp. 436-438, Feb. 2022.
3) A. Paidimarri et al.: “A high-linearity, 24–30 GHz RF, beamforming and frequency-conversion IC for scalable 5G phased arrays,” Proc. IEEE Radio Freq. Integr. Circuits Symp. (RFIC), pp. 103–106, Jun. 2021.
4) Y. Hasegawa et al.: “Compact and low-loss stripline bandpass filters made of liquid crystal polymer for n257 and n258 applications,” Proc. European Microw. Conf. (EuMC), pp. 437-440, Apr. 2022.
5) X. Gu et al.: “Antenna-in-package integration for a wide-band scalable 5G millimeter-wave phased-array module,” IEEE Microw. Wirelss Compon. Lett., vol. 31, no. 6, pp. 682–684, Jun. 2021.
6) T. W. Li et al.: “A continuous-mode harmonically tuned 19-to-29.5GHz ultra-linear PA supporting 18Gb/s at 18.4% modulation PAE and 43.5% peak PAE,” Proc. IEEE Int. Solid-State Circuit Conf. (ISSCC), pp. 410–412, Feb. 2018.
7) S. Shakib et al.: “A highly efficient and linear power amplifier for 28-GHz 5G phased array radios in 28-nm CMOS," IEEE Journal of Solid-State Circuits, vol. 51, no. 12, pp. 3020-3036, 2016.
8) C. Kamidaki et al.: “A 24–30 GHz power amplifier with >20-dBm Psat and <0.1-dB AM-AM distortion for 5G applications," Proc. Asia-Pacific Microw. Conf. (APMC), Nov. 2022.
9) C. Kamidaki et al.: “A 24–30 GHz power amplifier with >20-dBm Psat and <0.1-dB AM-AM distortion for 5G applications in 130-nm SiGe BiCMOS," IEICE Trans. Electron., vol.E106-C, no.11, pp. 625-634, Nov. 2023.
10) Y. W. Chang et al.: “A 28 GHz linear and efficient power amplifier supporting wideband OFDM for 5G in 28nm CMOS,” IEEE/MTT-S Int. Microw. Symp. (IMS) Dig., pp. 1093–1096, Aug. 2020.
11) T. C. Tsai et al.: “A linear and efficient power amplifier supporting wideband 64-QAM for 5G applications from 26 to 30 GHz in SiGe:C BiCMOS,” Proc. IEEE Radio Freq. Integr. Circuits Symp. (RFIC), pp. 127–130, July 2021.
12) T. Sugiura et al.: “25-GHz-band high efficiency stacked-FET power amplifier IC with adaptive controlled gate capacitor in 45-nm SOI CMOS,” Proc. IEEE Topical Conf. on RF/Microw. Power Amplifiers Wireless Radio Appl. (PAWR), pp. 26-28, Jan. 2022.
13) International Technology Roadmap for Semiconductors 2001, System Drivers Edition, p. 10.